

# Coupling of Ligand Binding and Dimerization of Helix-Loop-Helix Peptides: Spectroscopic and Sedimentation Analyses of Calbindin D<sub>9k</sub> EF-Hands

Karin Julenius,<sup>1</sup> James Robblee,<sup>2</sup> Eva Thulin,<sup>1</sup> Bryan E. Finn,<sup>1</sup> Robert Fairman,<sup>2</sup> and Sara Linse<sup>1\*</sup>

<sup>1</sup>Department of Biophysical Chemistry, Lund University, Lund, Sweden

<sup>2</sup>Department of Molecular, Cellular and Developmental Biology, Haverford College, Haverford, Pennsylvania

**ABSTRACT** Isolated Ca<sup>2+</sup>-binding EF-hand peptides have a tendency to dimerize. This study is an attempt to account for the coupled equilibria of Ca<sup>2+</sup>-binding and peptide association for two EF-hands with strikingly different loop sequence and net charge. We have studied each of the two separate EF-hand fragments from calbindin D<sub>9k</sub>. A series of Ca<sup>2+</sup>-titrations at different peptide concentrations were monitored by CD and fluorescence spectroscopy. All data were fitted simultaneously to both a complete model of all possible equilibrium intermediates and a reduced model not including dimerization in the absence of Ca<sup>2+</sup>. Analytical ultracentrifugation shows that the peptides may occur as monomers or dimers depending on the solution conditions. Our results show strikingly different behavior for the two EF-hands. The fragment containing the N-terminal EF-hand shows a strong tendency to dimerize in the Ca<sup>2+</sup>-bound state. The average Ca<sup>2+</sup>-affinity is 3.5 orders of magnitude lower than for the intact protein. We observe a large apparent cooperativity of Ca<sup>2+</sup> binding for the overall process from Ca<sup>2+</sup>-free monomer to fully loaded dimer, showing that a Ca<sup>2+</sup>-free EF-hand folds upon dimerization to a Ca<sup>2+</sup>-bound EF-hand, thereby presenting a preformed binding site to the second Ca<sup>2+</sup>-ion. The C-terminal EF-hand shows a much smaller tendency to dimerize, which may be related to its larger net negative charge. In spite of the differences in dimerization behavior, the Ca<sup>2+</sup> affinities of both EF-hand fragments are similar and in the range lgK = 4.6–5.3. *Proteins* 2002;47:323–333.

© 2002 Wiley-Liss, Inc.

**Key words:** thermodynamic linkage; association-driven folding; four-helix bundle

## INTRODUCTION

The Ca<sup>2+</sup> ion is an important messenger used in many signalling pathways in biological systems, depending on specific Ca<sup>2+</sup>-binding proteins. Common to many of these proteins is a Ca<sup>2+</sup>-binding motif called EF-hand, with a characteristic helix-loop-helix fold. The Ca<sup>2+</sup>-ion is coordinated by carbonyl and carboxyl oxygens, often complemented with a water molecule. EF-hand motifs normally occur in pairs with the two Ca<sup>2+</sup>-binding loops coupled through a short antiparallel  $\beta$  sheet. A pair may constitute

a globular domain or be part of a larger entity. Pairing of sites allows for cooperative Ca<sup>2+</sup>-binding, which enables Ca<sup>2+</sup>-controlled activities to turn on or off over a narrow range of free Ca<sup>2+</sup> concentration. The EF-hand motif was first discovered in the crystal structure of parvalbumin,<sup>1</sup> and over 30 distinct subfamilies of EF-hand proteins have been described.<sup>2</sup> The subfamilies are often divided into two groups according to the effect of Ca<sup>2+</sup>-binding on the protein structure. The Ca<sup>2+</sup>-sensor proteins, such as calmodulin and troponin C, are inactive at low Ca<sup>2+</sup> concentrations (10<sup>-7</sup>–10<sup>-8</sup> M) and undergo substantial conformational changes when Ca<sup>2+</sup> is bound at high Ca<sup>2+</sup> concentrations (10<sup>-5</sup>–10<sup>-6</sup> M), leading to activation of target enzymes and a cellular response. The conformational effect of Ca<sup>2+</sup>-binding is much smaller in the other group containing proteins involved in Ca<sup>2+</sup> buffer and transport functions.

The presence of two or more Ca<sup>2+</sup>-binding sites in one protein with positive cooperativity makes it difficult to assess the site-specific effects of mutations or changes in solution conditions. To overcome this problem and to study the effects of protein truncation, researchers have studied single, isolated EF-hands, obtained either by protein cleavage or by peptide synthesis. In earlier studies, peptides with different lengths<sup>3,4</sup> and different amino acid sequences<sup>5–9</sup> have been compared with regard to secondary structure content and apparent Ca<sup>2+</sup> affinity. The latter has been extracted from the data in a simplified way, without regard to peptide association. Studies on EF-hand III from skeletal troponin C have expanded our knowledge greatly, since this was the first case in which an isolated EF-hand was shown to dimerize in the presence of Ca<sup>2+</sup>.<sup>10–12</sup> The same behavior was later found for several other EF-hands.<sup>13–15</sup> The coupling of dimerization and Ca<sup>2+</sup> binding makes it necessary to carefully control the peptide concentration when performing Ca<sup>2+</sup> titration experiments on single EF-hands. If differences in titration behavior are found with different peptide sequences, this

Karin Julenius's present address is Bioinvent Therapeutic AB, S-223 70 Lund, Sweden.

\*Correspondence to: Sara Linse, Biophysical Chemistry, Lund University Chemical Centre, PO Box 124, S-221 00 Lund, Sweden. E-mail: sara.linse@bpc.lu.se

Received 6 July 2001; Accepted 30 November 2001



give protein stock solutions, which were diluted to give the desired protein concentrations. Protein concentrations were confirmed by acid hydrolysis and amino acid analysis. The buffer used was 2 mM Tris/HCl, pH 7.5.  $\text{Ca}^{2+}$  solutions were made from dissolving  $\text{CaCl}_2$  in buffer. EDTA solutions were made by dissolving Titriplex III from Merck (Darmstadt, Germany) in buffer and adjusting the pH to 7.5 with KOH. The residual  $\text{Ca}^{2+}$  contents of the protein fragments and the buffer were determined using a chromophoric  $\text{Ca}^{2+}$  chelator (Quin-2) and UV absorbance spectroscopy.

### CD Spectroscopy

The CD spectra were obtained using a Jasco J-720 spectropolarimeter with a Jasco PTC-343 Peltier type thermostatic cell holder. All data were collected at 25.0°C. Quartz cuvettes with path lengths of 1, 2, 4, or 10 mm were used. Only data for which the voltage of the photomultiplier was below 700 V was used (excludes the lower wavelengths at high concentrations due to high absorbance). At higher voltage, the photomultiplier of the instrument becomes saturated and the signal-to-noise ratio of the CD-signal deteriorates rapidly.

### Fluorescence Spectroscopy

The fluorescence spectra were obtained using a Perkin Elmer Luminescence Spectrometer LS 50 B connected to a Julabo F25 thermostatic water bath. All data were collected at 25.0°C. The EF1 sample was excited at 274 nm (Tyr) and the EF2 at 260 nm (Phe). The excitation slit was 3 nm and the emission slit 4 nm. Fluorescence cuvettes made of quartz with path lengths of 4×10 or 10×10 mm were used.

### Analytical Ultracentrifugation

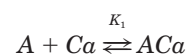
Concentrated stock solutions of the two EF-hands were prepared from freeze-dried material. Samples containing peptide, 2 mM Tris-HCl pH = 7.5, 0.1M KCl, and either 50  $\mu\text{M}$  EDTA or 4 mM  $\text{CaCl}_2$  (where specified) were prepared from stock solutions of each individual component. Reference samples were made in an identical fashion excluding the addition of peptide. Samples were analyzed using six channel, 12-mm path length charcoal-filled Epon cells enclosed by quartz windows. Sedimentation equilibrium experiments were performed at 25°C at rotor speeds of 30,000, 40,000, and 50,000 rpm using a Beckman Optima XL-A analytical ultracentrifuge with an An-60Ti rotor. Twenty absorbance scans were averaged. Solution densities were calculated using standard tables listing coefficients for the power series approximation of the change in density ( $\Delta\rho$ ) for individual components.<sup>20</sup> These  $\Delta\rho$ 's were then summed and added to the density of pure water at 25°C (0.997073 g/mL). Partial specific volumes for both EF-hand fragments were calculated from the weighted average of the partial specific volume of the individual amino acids.<sup>20</sup> The Nonlinear Least Squares Program (HID) obtained from the Analytical Ultracentrifugation Facility at the University of Connecticut was used for the curve fitting data analysis.

### Analysis of $\text{Ca}^{2+}$ Binding Data

The data analysis was carried out using the software MATLAB (The Math Works, Inc.). A MATLAB program was written using the Levenberg-Marquardt algorithm for least square fits.<sup>21</sup> The program, called LMFIT, allows simultaneous fitting of a large number functions and data sets so that one or more common constants may be determined with higher precision.

To correct for the use of different cuvettes, the CD signals were multiplied by a factor 10/d, where d is the path length in mm. The fluorescence data obtained in a 10 × 10 mm cuvette was corrected by division of a factor 1.30 to be comparable to the 4 × 10 mm cuvette data. This factor was obtained from several fluorescence measurement of identical samples in 4 × 10 mm and 10 × 10 mm cuvettes. The total peptide concentration,  $A_{\text{tot}}$ , at each titration point was calculated from  $A_0$  (the initial value of  $A_{\text{tot}}$ ) and the dilutions due to  $\text{Ca}^{2+}$  additions. The total  $\text{Ca}^{2+}$  concentration,  $Ca_{\text{tot}}$ , was calculated from the residual  $\text{Ca}^{2+}$  contents of the protein fragments and the buffer, the  $\text{Ca}^{2+}$  additions and the dilutions.

In a preliminary analysis, each titration curve was fitted independently, assuming no dimerization, to a single  $\text{Ca}^{2+}$ -binding constant,  $K_1$ . This was done to assess the quality of the data and the effect of protein concentration. This simple model will subsequently be referred to as the 2-state model.



$$K_1 = \frac{[ACa]}{[A][Ca]} \quad (1)$$

The total  $\text{Ca}^{2+}$  concentration,  $Ca_{\text{tot}}$ , is the sum of the concentrations of all calcium-containing species. In this case

$$Ca_{\text{tot}} = [Ca] + [ACa] \quad (2)$$

The total peptide concentration,  $A_{\text{tot}}$ , is the sum of the concentrations of all peptide-containing species. In this case

$$A_{\text{tot}} = [A] + [ACa] \quad (3)$$

Substitution for [ACa] in eq. (2) using eq. (1) and rearrangement gives

$$[Ca] = \frac{Ca_{\text{tot}}}{1 + K_1[A]} \quad (4)$$

Substitution for [ACa] in eq. (3) using eq. (1) and eq. (4) gives

$$A_{\text{tot}} = [A] + \frac{K_1[A]Ca_{\text{tot}}}{1 + K_1[A]} \quad (5)$$

Multiplication with  $(1 + K_1[A])$  and rearrangement gives

$$K_1[A]^2 + (1 + Ca_{\text{tot}}K_1 - A_{\text{tot}}K_1)[A] - A_{\text{tot}} = 0 \quad (6)$$

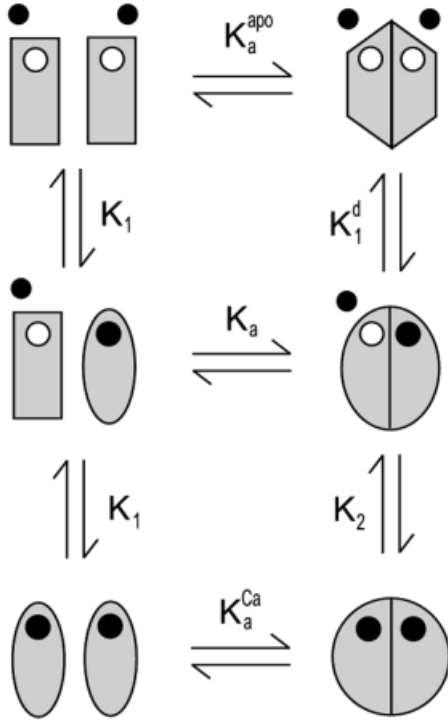


Fig. 3. The 5-state model including all possible dimerization and  $\text{Ca}^{2+}$ -binding events that can take place with an isolated EF-hand fragment. The 4-state model is obtained by omitting apo dimers and the equilibria described by association constants  $K_a^{\text{apo}}$  and  $K_1^{\text{d}}$ .

This quadratic equation may be solved analytically using the standard solution of quadratic equations. Only the positive root is valid, since  $[A]$  cannot be negative. The spectroscopic data are fitted using molar spectroscopic values for the apo form and the  $\text{Ca}^{2+}$ -loaded form:  $Y_{\text{apo}}$  and  $Y_{\text{Ca}}$ .

$$Y = Y_{\text{Ca}} + \frac{[A]}{A_{\text{tot}}} (Y_{\text{apo}} - Y_{\text{Ca}}) \quad (7)$$

CD and fluorescence spectroscopy are methods where dilution affects the signal and the peptide concentration change were accounted for by multiplying the right hand side of equation (7) with the ratio  $A_{\text{tot}}/A_0$ .

The fact that the errors vary in complicated ways with factors such as wavelength, path length, method, and concentration made careful assessment of the measurement errors necessary. The measurement errors were assumed to be absolute in the case of CD spectroscopy and to be relative in the case of fluorescence spectroscopy. To estimate the magnitude of the errors, a scaling factor was allowed to change until  $\chi^2$  was equal to the number of degrees of freedom. This was done for each titration separately, using the simple two-state model, and the errors were used in the fittings of the more complicated models.

In a more extensive analysis, a complete model of all possible equilibria as shown in Figure 3 was used. This model will subsequently be referred to as the 5-state model, because the peptide can exist in five different

states: apo monomer,  $\text{Ca}_1$ -monomer, apo dimer,  $\text{Ca}_1$ -dimer, or  $\text{Ca}_2$ -dimer. The corresponding equations are:

$$K_1 = \frac{[ACa]}{[A][Ca]} \quad (8)$$

$$K_a = \frac{[A_2Ca]}{[A][ACa]} \quad (9)$$

$$K_2 = \frac{[A_2Ca_2]}{[A_2Ca][Ca]} \quad (10)$$

$$K_a^{\text{Ca}} = \frac{[A_2Ca_2]}{[ACa]^2} \quad (11)$$

$$K_a^{\text{apo}} = \frac{[A_2]}{[A]^2} \quad (12)$$

$$K_1^{\text{d}} = \frac{[A_2Ca]}{[A_2][Ca]} \quad (13)$$

Hence,  $K_a$ ,  $K_a^{\text{apo}}$ , and  $K_a^{\text{Ca}}$  are dimerization constants, and  $K_1$ ,  $K_2$ , and  $K_1^{\text{d}}$  are  $\text{Ca}^{2+}$  association constants. Since the six equilibria (the two equilibria depicted in the left column of Figure 3 are actually the same equilibrium) are connected in a thermodynamic double cycle, it is only necessary to determine four of them [e.g., eqs. (8), (9), (10), and (12)]. To account for all the  $\text{Ca}^{2+}$ -bound species present, eq. (2) is modified into eq. (14).

$$Ca_{\text{tot}} = [Ca] + [ACa] + [A_2Ca] + 2[A_2Ca_2] \quad (14)$$

Substituting for the species  $[ACa]$ ,  $[A_2Ca]$  and  $[A_2Ca_2]$  using eqs. (8), (9), and (10) and rearranging we arrive at the following quadratic equation

$$2K_1K_aK_2[A]^2[Ca]^2 + (1 + K_1[A] + K_1K_a[A]^2)[Ca] - Ca_{\text{tot}} = 0 \quad (15)$$

Eq. (3) is modified to

$$A_{\text{tot}} = [A] + [ACa] + 2[A_2Ca] + 2[A_2Ca_2] + 2[A_2] \quad (16)$$

Substitution using eqs. (9), (10), (11), and (13) gives

$$A_{\text{tot}} = K_1[A][Ca] + 2K_1K_a[A]^2[Ca] + 2K_1K_aK_2[A]^2[Ca]^2 + 2K_a^{\text{apo}}[A]^2 \quad (17)$$

$[Ca]$  may be solved analytically from eq. (15). When this expression is used instead of  $[Ca]$  in eq. (17), it becomes impossible to solve analytically. Therefore, this is done numerically with a MATLAB command called `fzero`. This algorithm was originally written by T. Dekker and uses a combination of bisection, secant, and inverse quadratic interpolation methods.<sup>22</sup> The various peptide species are assumed to contribute linearly to the CD or fluorescence signal.

$$Y_A = m_A[A] \quad (18)$$

$$Y_{ACa} = m_{ACa}[ACa] \quad (19)$$

$$Y_{A_2Ca} = m_{A_2Ca}[A_2Ca] \quad (20)$$

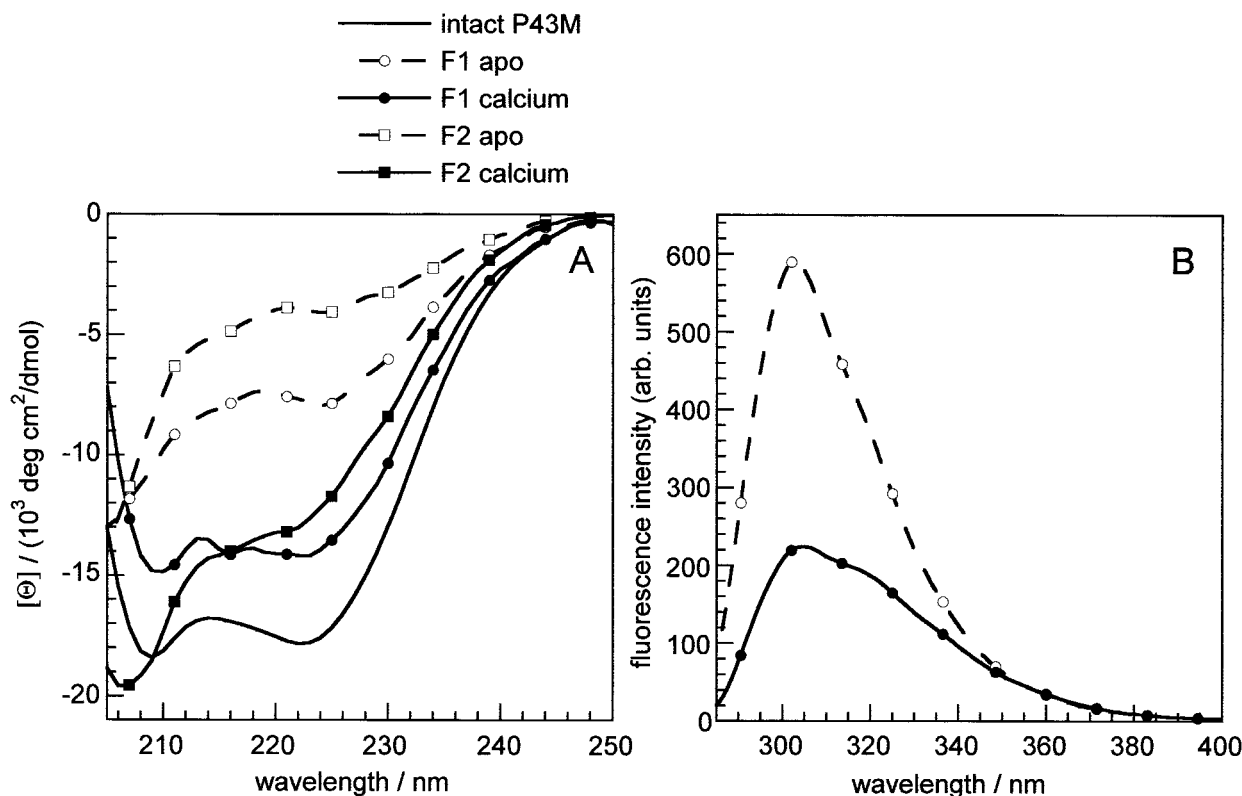


Fig. 4. CD and fluorescence spectra of the isolated EF-hands from calbindin  $D_{9k}$ . **A:** The mean residue ellipticity,  $[\Theta]$ , for EF1 (30  $\mu\text{M}$ ) and EF2 (43  $\mu\text{M}$ ) as compared to intact calbindin  $D_{9k}$ . The same samples were used for both the apo and  $\text{Ca}^{2+}$  spectra. First, 50  $\mu\text{M}$  EDTA was added and the apo spectra were obtained. Then 10 mM  $\text{CaCl}_2$  was added and the  $\text{Ca}^{2+}$  spectra were obtained. **B:** Fluorescence emission spectra of EF1 (43  $\mu\text{M}$ ) in the absence and presence of 2.5 mM  $\text{CaCl}_2$ .

$$Y_{A_2Ca_2} = m_{A_2Ca_2}[A_2Ca_2] \quad (21)$$

$$Y_{A_2} = m_{A_2}[A_2] \quad (22)$$

The spectroscopic signal is obtained by summation of the contributions of the different peptide species and addition of the background signal,  $b$ .

$$Y = Y_A + Y_{ACa} + Y_{A_2Ca} + Y_{A_2Ca_2} + Y_{A_2} + b \quad (23)$$

Since evidence for the existence of an apo multimeric state has been found in one case only,<sup>23</sup> attempts were also made to fit the data to a simplified model not including the apo dimer. This model will subsequently be referred to as the 4-state model. Eqs. (16), (17), and (23) were simplified accordingly into eqs. (24), (25), and (26), respectively.

$$A_{\text{tot}} = [A] + [ACa] + [A_2Ca] + [A_2Ca_2] \quad (24)$$

$$A = K_1[A][Ca] + 2K_1K_a[A]^2[Ca] + 2K_1K_aK_2[A]^2[Ca]^2 \quad (25)$$

$$Y = Y_A + Y_{ACa} + Y_{A_2Ca} + Y_{A_2Ca_2} + b \quad (26)$$

Several data sets were used simultaneously to obtain better precision in the equilibrium binding constants using the multiple function option in LMFIT. For EF1, CD data at different wavelengths were combined with each other and with fluorescence data at different wavelengths by allowing the constants  $m_A$ ,  $m_{ACa}$ ,  $m_{A_2Ca}$ ,  $m_{A_2Ca_2}$ , and  $b$  to

be wavelength-specific, but keeping  $K_1$ ,  $K_a$ , and  $K_2$  constant for all wavelengths. For EF2, the data for different concentrations and different wavelengths was combined by assigning individual values of  $Y_{\text{apo}}$  and  $Y_{\text{Ca}}$  to each combination of concentration and wavelength, but letting  $K_1$  be common for all data sets. In the text, the binding constants are discussed as  $\lg K$  ( $\lg K = {}^{10}\log K = -pK$ ).

## RESULTS

### CNBr Cleavage and Isolation of Fragments

The calbindin  $D_{9k}$  Pro43→Met mutant (P43M) was cleaved by CNBr to produce the single EF-hand fragments EF1 (residues 1–43) and EF2 (residues 44–75). The two fragments have different net charges (−1 for EF1 and −6 for EF2) and could, therefore, be separated from each other using ion exchange chromatography in the presence of EDTA, followed by desalting on a G25 gel filtration column. The yields of pure desalted fragments were 16–19 mg of EF1 and 8–12 mg of EF2 when 50 mg intact protein was cleaved.

### CD Spectra

The CD spectra of the two EF-hand fragments of calbindin  $D_{9k}$  in the presence and absence of  $\text{Ca}^{2+}$  are seen in Figure 4(A) together with the CD spectrum of the intact protein. The CD signals of both EF1 and EF2 change

**TABLE I. Single Species Analysis of Sedimentation Equilibrium Data for EF2<sup>†</sup>**

Sample conditions	Rotor speed (rpm)			
	30,000	40,000	50,000	Global
42.6 $\mu$ M EF2, Apo	5,000 $\pm$ 600	3,800 $\pm$ 400	2,900 $\pm$ 200	3,100 $\pm$ 200
42.6 $\mu$ M EF2, Apo, KCl	11,400 $\pm$ 1,100	7,600 $\pm$ 700	5,800 $\pm$ 300	6,400 $\pm$ 500
42.6 $\mu$ M EF2, CaCl <sub>2</sub>	10,000 $\pm$ 900	9,900 $\pm$ 400	9,300 $\pm$ 300	9,500 $\pm$ 300
42.6 $\mu$ M EF2, CaCl <sub>2</sub> , KCl	10,700 $\pm$ 700	10,000 $\pm$ 400	9,200 $\pm$ 300	9,500 $\pm$ 300

<sup>†</sup>A single species analysis treats the molecular weight as a variable in the curve fitting analysis. The global analysis analyzes the data from the three rotor speeds simultaneously. Molecular mass in Daltons; the theoretical monomer molecular weight is 3,674.0 Daltons.

substantially upon Ca<sup>2+</sup> addition, making it possible to use CD spectroscopy as a probe of Ca<sup>2+</sup> binding. The Ca<sup>2+</sup>-form of EF1 yields a spectrum typical of an  $\alpha$ -helical structure. It closely resembles the spectrum of the intact protein, although the magnitude of the signal is smaller. This is an indication that the Ca<sup>2+</sup>-form of EF1 has a secondary structure similar to the highly helical calbindin D<sub>9k</sub>. The reduction in signal compared to the intact protein may be explained by mere fraying of helices, without reduction of the number of helical residues, according to a theoretical study by Hirst and Brooks.<sup>24</sup> The CD spectrum of EF1 may be consistent with a symmetric dimer structure like the one found for EF-hand III of chicken troponin C<sup>12</sup>. The Ca<sup>2+</sup>-form of EF2 also yields a spectrum with substantial signal intensity, but the ratio of the intensities at 222 and 208 nm is smaller than for EF1, which may suggest a lower degree of  $\alpha$ -helical structure. The CD signals of the Ca<sup>2+</sup>-free (apo) forms, especially for EF2, are much weaker than the signals for the Ca<sup>2+</sup> forms, suggesting that Ca<sup>2+</sup> stabilizes the secondary structure elements and induces folding.

### Fluorescence Spectra

EF1 contains one tyrosine and two phenylalanine residues, and the tyrosine fluorescence spectra in the presence and absence of Ca<sup>2+</sup> are shown in Figure 4(B). The spectra reveal a large decrease in fluorescence signal upon calcium binding, which may be monitored during a Ca<sup>2+</sup>-titration experiment. Since folding of proteins generally results in decreased amounts of tyrosine emission,<sup>25</sup> the large decrease in fluorescence signal upon Ca<sup>2+</sup> binding may be taken as an additional indication of a Ca<sup>2+</sup>-induced folding process. EF2 contains only 3 aromatic residues, all of which are phenylalanines. The fluorescence of EF2 in the presence and absence of calcium was investigated, but the signal was overall very weak and the differences between the spectra of the Ca<sup>2+</sup> and apo forms were very small (data not shown).

### Analytical Ultracentrifugation of EF2

Sedimentation equilibrium analytical ultracentrifugation was performed to probe the homo-oligomerization state of EF2 in both the absence and presence of Ca<sup>2+</sup>. In the absence of calcium, the monomer molecular weight (3,674.0 Da) is underpredicted (Table I). This is likely due to electrostatic repulsion of the highly charged apo form of EF2 ( $Z = -6$ ). Thus, at 42.6  $\mu$ M, apo EF2 is completely monomeric with no evidence for self-association. In the

presence of 0.1M KCl, apo EF2 shows significant self-association as reflected in the elevated molecular weight (6,400  $\pm$  500; obtained from global fits using all three concentrations simultaneously). The observed trend of decreasing apparent molecular weight with increasing rotor speed, which is an evidence for multiple species, further supports this conclusion.

The global molecular weight of EF2 in the presence of Ca<sup>2+</sup> is intermediate between a dimer and trimer. Thus, there is evidence for association above a dimer in the presence of a significant excess of Ca<sup>2+</sup>.

### Ca<sup>2+</sup> Titration of EF2

One series of Ca<sup>2+</sup>-titrations was performed on EF2 and monitored by CD at 210, 215, 220, 225, and 230 nm. The 220-nm data is shown in Figure 5(A). EF2 was titrated with Ca<sup>2+</sup> under a wide range of peptide concentrations (1.7–250.4  $\mu$ M), and attempts to fit the individual titration curves using a single Ca<sup>2+</sup>-binding constant yielded essentially the same result for all curves. Attempts to fit the titration data to the more complex 4-state and/or 5-state models (Fig. 3) gave no significant improvement over the 2-state model, and all binding constants except  $K_1$  were completely undefined with the errors larger than the obtained values. Therefore, all titrations, including all combinations of concentrations and wavelengths, were fitted simultaneously to a common  $K_1$ -value using the 2-state model while  $Y_{Ca}$  and  $Y_{apo}$  were allowed to be titration-specific. Data with total Ca<sup>2+</sup> concentration above 1 mM were discarded before the final fitting because the increased ion strength may affect the equilibria of the highly charged EF2 ( $Z = -6$  in the apo form). The resulting fit is shown as the solid line in Figure 5(A). It yielded the association constant  $\lg K_1 = 4.620 \pm 0.004$ . A deviation from the fitted curves can be seen at the highest EF2 concentrations (166.9 and 250.4  $\mu$ M), probably due to influence of dimerization at these peptide concentrations. When plotting the degree of Ca<sup>2+</sup> saturation vs. the free Ca<sup>2+</sup> concentration [Fig. 5(B)], it is clear that overall the EF2 data is consistent with a single binding constant as the midpoint free Ca<sup>2+</sup> concentration is the same for all titrations. The value of  $K_1$  corresponds to a dissociation constant of  $24.0 \pm 0.2 \mu$ M, which is equal to the midpoint in the transformed binding curves shown in Figure 4(B).

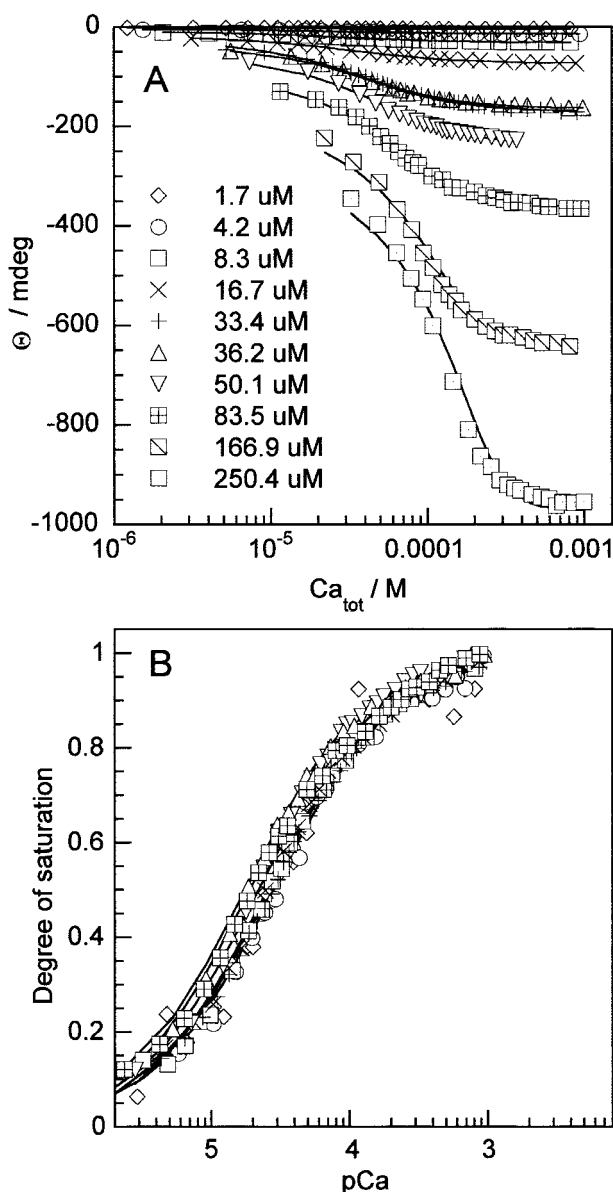


Fig. 5. **A:**  $\text{Ca}^{2+}$  titrations of EF2 as measured by CD spectroscopy at 220 nm. The solid line was obtained by least-squares fitting simultaneously to all data using the 2-state model. **B:** The data and fitted curve in A for 1.7–83.5  $\mu\text{M}$  EF2 transformed to the degree of  $\text{Ca}^{2+}$  saturation as a function of free  $\text{Ca}^{2+}$ .

### Analytical Ultracentrifugation of EF1

Sedimentation equilibrium analytical ultracentrifugation was performed to probe the homo-oligomerization state of EF1 in both the absence and presence of  $\text{Ca}^{2+}$ . The apparent molecular weight in the absence of  $\text{Ca}^{2+}$  is higher than that expected for a monomer across the eightfold concentration range studied, from 39 to 312  $\mu\text{M}$  (Table II). However, the apparent molecular weight is independent of concentration, contrary to the results expected for a self-associating system in solution. Additionally, no trend of decreasing molecular weight with increasing rotor speed is observed, suggesting that a single

species is present in solution. Taken together, these results suggest that EF1 is monomeric in the absence of  $\text{Ca}^{2+}$ .

In the presence of 4 mM  $\text{Ca}^{2+}$ , the molecular weight is only slightly elevated above that of a dimer (9,757.2 Da). Modeling higher order association states above that of a dimer did not improve the fit of the model to the data (data not shown). The elevated observed molecular weights in both conditions could be due to ill-determined values for the calculated peptide partial specific volumes or solvent densities. Equally plausible is the possibility that a small amount of irreversible aggregation formed in the concentrated stock solution. Nevertheless, the results strongly correlate with an oligomerization state of a monomer and dimer in the absence and presence of  $\text{Ca}^{2+}$ , respectively.

### $\text{Ca}^{2+}$ Titration of EF1

Two series of  $\text{Ca}^{2+}$ -titrations were performed on EF1 with peptide concentrations ranging from 1.6 to 86  $\mu\text{M}$ . The first titration series was monitored with CD at 222 nm and is shown in Figure 6(A). The second was monitored with CD at 205, 210, 215, 220, 225, and 230 nm and with fluorescence at 295, 300, 303, 305, 310, 315, 320, 325, and 330 nm. In Figure 6(B), 303-nm fluorescence data are shown as an example. Attempts to fit each individual titration curve to a single apparent  $\text{Ca}^{2+}$ -binding constant did not yield consistent results and instead showed a strong correlation between fragment concentration and apparent  $\text{Ca}^{2+}$  affinity. Therefore, all titrations were fitted simultaneously allowing for dimerization of the peptides. A fit to the  $\text{Ca}^{2+}$ -titration data using the 4-state (no apo dimers, Fig. 3) yields  $\lg K_1 = 4.41 \pm 0.01$ ,  $\lg K_a = 4.67 \pm 0.03$ , and  $\lg K_2 = 4.95 \pm 0.01$ . This fit is shown as a solid line in Figure 6(A,B) for the 222-nm CD data and the 303-nm fluorescence data, respectively. The association constant for dimerization of two  $\text{Ca}^{2+}$ -bound EF1 can be calculated from the three fitted constants as  $\lg K_a(\text{Ca}) = \lg K_a + \lg K_2 - \lg K_1 = 5.21$ . The corresponding fit of the 5-state model (apo dimers allowed) looks almost exactly the same to the eye (curve not shown), but a slightly lower  $\chi^2$  is found. The results of the analytical ultracentrifugation suggest that  $\text{Ca}^{2+}$ -bound EF1 is dimeric whereas the apo form is monomeric, and therefore supports the 4-state model. For comparison of the titrations at different EF1 concentrations, the degree of saturation was plotted vs. the free  $\text{Ca}^{2+}$  concentration. The midpoint of the  $\text{Ca}^{2+}$ -titration curves is clearly dependent on peptide concentration, as expected from the preliminary fits of the individual titration curves, which yielded a concentration-dependent apparent  $\text{Ca}^{2+}$  affinity.

Since two independent titration series were available and since for the last titration series, two different methods were used (CD and fluorescence), fitting to different sub-sets of the data gave us an idea of how well determined the different association constants are. Overall, the  $\text{Ca}^{2+}$ -binding constants were better determined than the dimerization constant(s) for both models.

**TABLE II. Single Species Analysis of Sedimentation Equilibrium Data for EF1<sup>†</sup>**

Sample conditions	Peptide ( $\mu\text{M}$ )	Rotor speed (rpm)			
		30,000	40,000	50,000	Global
156 $\mu\text{M}$ EF1, Apo	39	6,200 $\pm$ 800	6,500 $\pm$ 700	6,200 $\pm$ 400	6,200 $\pm$ 400
	156	6,500 $\pm$ 600	6,600 $\pm$ 500	6,400 $\pm$ 200	6,400 $\pm$ 300
	312	6,300 $\pm$ 800	6,900 $\pm$ 700	5,500 $\pm$ 600	6,100 $\pm$ 600
156 $\mu\text{M}$ EF1, $\text{CaCl}_2$	39	11,200 $\pm$ 100	10,400 $\pm$ 400	10,100 $\pm$ 300	10,200 $\pm$ 300
	156	11,300 $\pm$ 700	10,700 $\pm$ 400	10,100 $\pm$ 200	10,300 $\pm$ 200
	312	10,000 $\pm$ 100	10,100 $\pm$ 700	9,200 $\pm$ 600	9,700 $\pm$ 500

<sup>†</sup>A single species analysis treats the molecular weight as a variable in the curve fitting analysis. The Global analysis analyzes the data from the three rotor speeds simultaneously. Molecular mass in Daltons; the theoretical monomer molecular weight is 4878.6 Daltons. All data sets from the three peptide concentrations were analyzed simultaneously. The global molecular weight is not dependent on peptide concentration, thus this analysis is valid.

## DISCUSSION

The ability of EF-hand peptides to form homodimers or higher oligomers makes it necessary to analyze  $\text{Ca}^{2+}$ -binding data in terms of the coupled equilibria of  $\text{Ca}^{2+}$  binding and association. Furthermore, the analysis is greatly facilitated if another method, like analytical ultracentrifugation, can provide independent information on the oligomerization number and whether oligomers can be formed both in the absence and presence of  $\text{Ca}^{2+}$ . In the present work, we have attempted to resolve these questions by combining data from analytical ultracentrifugation and  $\text{Ca}^{2+}$  titrations followed by optical spectroscopy.

### EF1

The N-terminal EF-hand in calbindin  $\text{D}_{9k}$ , EF1, does not agree with the consensus sequence. The loop accommodates two extra residues and  $\text{Ca}^{2+}$  coordination is mainly via backbone carbonyls. In addition, the net charge of EF1 is low ( $-1$  without  $\text{Ca}^{2+}$  and  $+1$  with  $\text{Ca}^{2+}$  bound), although there are several negatively charged residues in and around the  $\text{Ca}^{2+}$ -binding site. In the intact protein, the N-terminal site is less flexible than the C-terminal site. This is observed as lower rates of backbone fluctuation<sup>26</sup> and a stringent selection for  $\text{Ca}^{2+}$  over other mono-, di- and trivalent metal ions<sup>27,28</sup>.

The analytical ultracentrifugation results imply that EF1 is monomeric in the absence of calcium and dimeric in the presence of  $\text{Ca}^{2+}$ . This suggests that the 4-state model, which neglects dimerization in the apo state, is of sufficient complexity for analysis of the  $\text{Ca}^{2+}$  titrations. We may then conclude that for EF1, the first  $\text{Ca}^{2+}$  ion binds to a monomer with an affinity of  $\lg K_1 = 4.41$ . The  $\text{Ca}^{2+}$ -bound EF1 may then associate with another  $\text{Ca}^{2+}$ -bound EF1 with an association constant of  $\lg K_a(\text{Ca}) = 5.21$ . Alternatively, it may associate with an apo EF1 ( $\lg K_a = 4.67$ ), and a second  $\text{Ca}^{2+}$  ion may bind to the dimer with an affinity of  $\lg K_2 = 4.95$ . Using the four association constants, the concentrations of the four species EF1 apo, EF1Ca, EF1<sub>2</sub>Ca, and EF1<sub>2</sub>Ca<sub>2</sub> may be calculated as a function of total  $\text{Ca}^{2+}$ , as shown in Figure 7 for two different EF1 concentrations (1 and 100  $\mu\text{M}$ ). At low  $\text{Ca}^{2+}$  concentration ( $< 1 \mu\text{M}$ ), there is no difference between the two cases, but as  $\text{Ca}^{2+}$  is added, the main species formed at 1  $\mu\text{M}$  EF1 is the  $\text{Ca}^{2+}$ -bound monomer, with little accumu-

lation of EF1<sub>2</sub>Ca<sub>2</sub>. At 100  $\mu\text{M}$  EF1, there is an accumulation of an EF1<sub>2</sub>Ca intermediate between 10 and 100  $\mu\text{M}$   $\text{Ca}^{2+}$ , which is then converted to mainly EF1<sub>2</sub>Ca<sub>2</sub> and some EF1Ca.

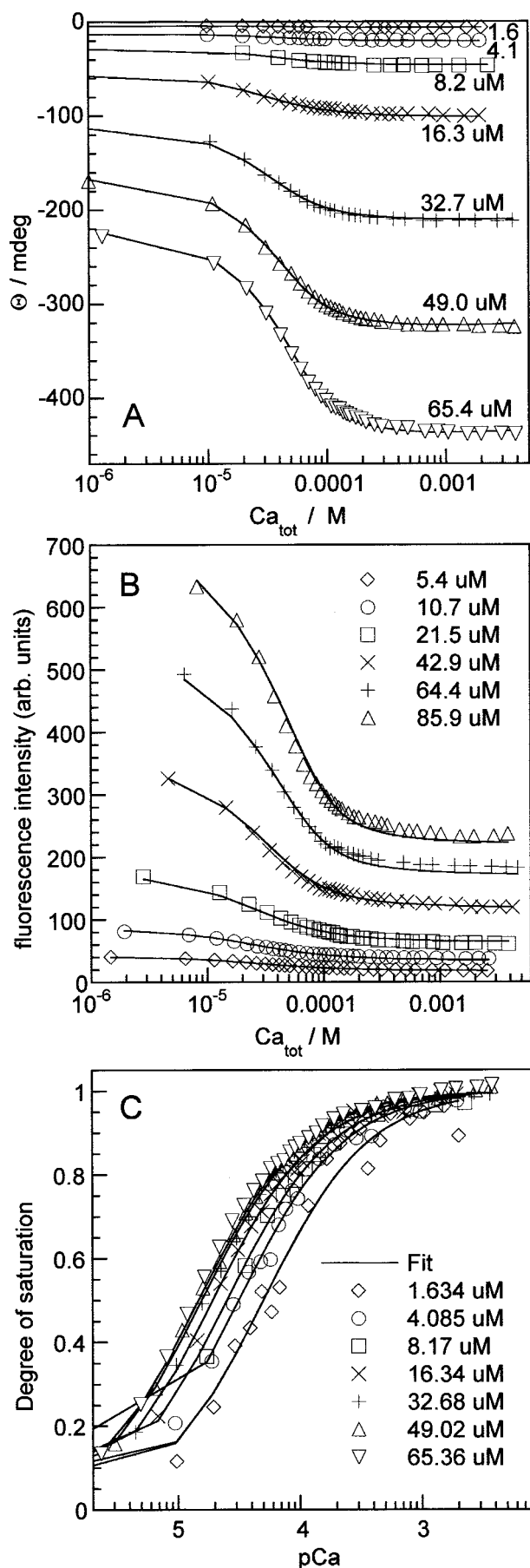
For EF1, which dimerizes only with calcium bound, it is evident that there is a strong coupling between  $\text{Ca}^{2+}$  binding, folding, and association of the EF-hand.

### EF2

The C-terminal EF-hand in calbindin  $\text{D}_{9k}$ , EF2, is a standard EF-hand with all the features expected from the consensus sequence. The net charge of EF2 is  $-6$  in the apo state and  $-4$  with  $\text{Ca}^{2+}$  bound. The C-terminal site uses mainly side-chain carboxylates to coordinate  $\text{Ca}^{2+}$ , and can therefore adjust the coordination sphere to accommodate a number of different divalent metal ions like  $\text{Cd}^{2+}$ ,  $\text{Mg}^{2+}$ ,  $\text{Mn}^{2+}$ , and also the trivalent lanthanide ions like  $\text{Lu}^{3+}$ ,  $\text{Eu}^{3+}$ , and many others.<sup>26-28</sup>

The apo form of EF2 is clearly a monomer in the absence of added salt. The analytical ultracentrifugation data underpredicts the monomer molecular weight, an indication of measurable electrostatic repulsion. Addition of  $\text{Ca}^{2+}$  and/or KCl seems to promote dimerization of the peptide. In contrast to EF1, very similar apparent  $\text{Ca}^{2+}$ -binding constants were obtained with different concentrations of the EF2 peptide. Hence, under the conditions of the  $\text{Ca}^{2+}$  titrations, dimerization does not influence the  $\text{Ca}^{2+}$  affinity of EF2. This may seem unexpected, because the high net negative charge of an EF2 homodimer would provide a very strong electrostatic attraction for  $\text{Ca}^{2+}$  ions. However, electrostatic repulsion between the two EF2 chains in the homodimer may prevent an optimal arrangement of the two  $\text{Ca}^{2+}$  loops. In earlier experiments, it was observed that the  $\text{Ca}^{2+}$  affinity is reduced in a predictable way when the net charge of intact calbindin  $\text{D}_{9k}$  is changed from  $-7$  to  $-6$ ,  $-5$ , or  $-4$  through site-directed mutagenesis.<sup>29,30</sup> However, when the net charge is changed to  $-8$ , as in either of the three single mutants N21D, Q22E, and N56D, the effect is either a decrease, or only a small increase, in  $\text{Ca}^{2+}$  affinity,<sup>31,32</sup> suggesting that when the negative charge becomes too large, structural destabilization leads to effects opposing the affinity gain resulting from an increased electrostatic attraction of  $\text{Ca}^{2+}$ .





Unfavorable electrostatic interactions between EF2 monomers in the apo form seem to prevent dimerization at low ionic strength. As discussed previously, the presence of salt increases the dimerization constant of apo EF2. In the presence of  $\text{Ca}^{2+}$ , dimers are observed both in the absence or presence of added KCl. However, the CD spectrum [Fig. 4(A)] suggests that the dimers do not have as well-defined helix-loop-helix structure as the intact protein and  $\text{Ca}^{2+}$ -bound EF1 homodimer.

### Cooperativity of Calcium Binding

In a system containing two  $\text{Ca}^{2+}$ -binding sites, there is a possibility for cooperativity between the sites, i.e., binding of the first  $\text{Ca}^{2+}$ -ion may change the affinity for the second ion. Cooperativity is most readily quantitated in a symmetric system with two identical sites. There seems to be no cooperativity in the EF2 system as the data are well fitted by a single apparent  $\text{Ca}^{2+}$ -binding constant. However, EF1 deserves a closer analysis. If we focus on the consecutive process ( $\text{Ca}^{2+}$  binding to monomer)–(dimerization)–( $\text{Ca}^{2+}$  binding to the empty second site in the dimer), an apparent cooperativity may be calculated from the ratio of  $K_2$  and  $K_1$ , as  $\Delta\Delta G = -RT \ln(K_2/K_1) = -3.1 \text{ kJ/mol}$ . There is hence a positive cooperativity ( $\Delta\Delta G < 0$ ), and the second  $\text{Ca}^{2+}$  ion is bound with a higher affinity than the first ( $K_2/K_1 = 3.5$ ). The degree of cooperativity is about half of that in the intact protein ( $\Delta\Delta G = -8.2 \text{ kJ/mol}^{33}$ ). The cooperativity observed for EF1 may arise from the fact that  $\text{Ca}^{2+}$  binding induces folding of the EF-hand (observed by CD spectroscopy), and this is at least partly propagated to its dimerization partner. In general, a large entropic contribution to the  $\text{Ca}^{2+}$  affinity for a protein or peptide comes from the release of water molecules from the first hydration shell of the solvated  $\text{Ca}^{2+}$  ion.  $\text{Ca}^{2+}$  binding is also promoted by electrostatic interactions and preformation of the binding site, while the affinity is reduced by conformational changes driven by the  $\text{Ca}^{2+}$  binding event (for review see Linse and Forsén<sup>34</sup>). Binding of the first  $\text{Ca}^{2+}$  ion to one EF1 peptide promotes dimerization with and folding of another EF1 copy, such that the second  $\text{Ca}^{2+}$  ion can more or less simply “pop in.” While both ions may get all the benefits of water release and interactions in the  $\text{Ca}^{2+}$  bound state, the first one has to pay most of the penalty of driving the conformational change. The first step will, therefore, display a lower  $\text{Ca}^{2+}$  affinity than the second, and the result is positive cooperativity.

### Comparison to Other EF-Hand Peptides

$\text{Ca}^{2+}$  binding data have been reported for a number of single EF-hand peptides, and the apparent affinities are

Fig. 6.  $\text{Ca}^{2+}$  titrations of EF1. **A**: The first series of titrations as monitored by CD spectroscopy at 222 nm. The solid line was obtained by least-squares fitting simultaneously to all data using the 4-state model. **B**: The second series of titrations as monitored by fluorescence spectroscopy at 303 nm. The solid line was obtained by least-squares fitting simultaneously to all data using the 4-state model. **C**: The data and fitted curve shown in A transformed to degree of  $\text{Ca}^{2+}$  saturation vs. the free  $\text{Ca}^{2+}$  concentration,  $[\text{Ca}]$ .

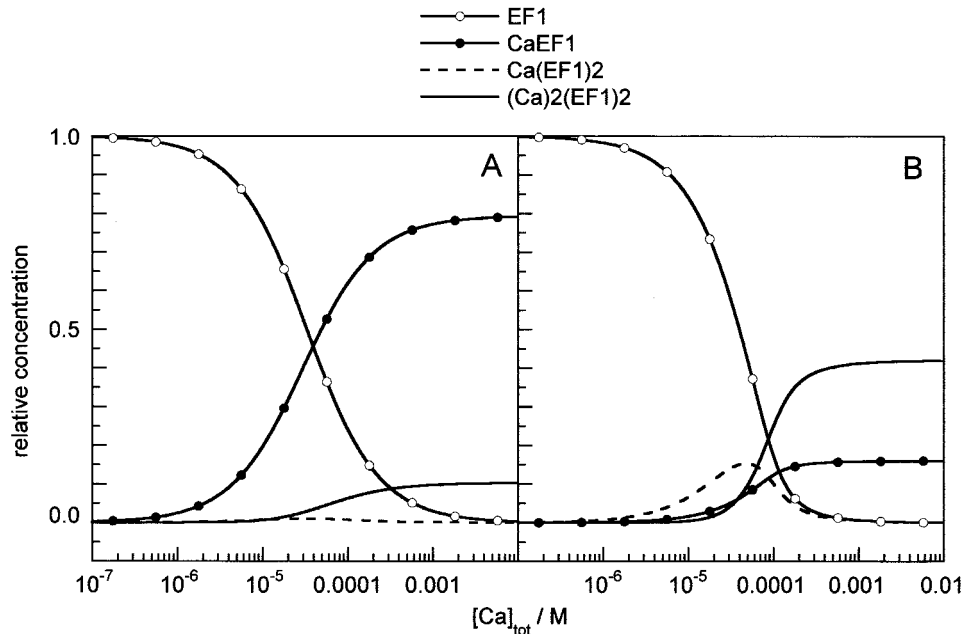


Fig. 7. Relative concentrations of EF1 apo, EF1Ca, EF<sub>1</sub><sub>2</sub>Ca, and EF<sub>1</sub><sub>2</sub>Ca<sub>2</sub> as a function of total Ca<sup>2+</sup> concentrations, [Ca]<sub>tot</sub>, calculated using the fitted association constants of the 4-state model for a total EF1-concentration of 1 μM (A) and 100 μM (B).

usually in the  $10^3$ – $10^5$  M<sup>-1</sup> range. Among the more careful studies are those of EF-hand III from troponin C (net charge of  $-6$  in the Ca<sup>2+</sup> form) in which attempts were made to account for the coupled equilibria of Ca<sup>2+</sup> binding and dimerization.<sup>35</sup> One-dimensional NMR-spectra were obtained during one Ca<sup>2+</sup> titration experiment with constant peptide concentration and one series of dilution experiments with constant Ca<sup>2+</sup>:peptide concentration ratio; in total 27 data points. Theoretical results for a large number of different combinations of binding constants were calculated and the combination of constant values that yielded the lowest standard deviation between calculated and experimental data was chosen. This procedure yielded association constants of  $\lg K_1 = 5.5$  for the first Ca<sup>2+</sup> and  $\lg K_a = 5.0$  for the dimerization, but the binding of the second Ca<sup>2+</sup> ion to the dimer was found to be too weak to be determined.<sup>35</sup> The fact that the affinity for the first Ca<sup>2+</sup> ion was much higher than for the second implies a strong negative cooperativity in the troponin C EF-hand III system. Clearly, this system behaves differently than both EF1 and EF2 from calbindin D<sub>9k</sub>.

#### Comparison to the EF1-EF2 Heterodimer

Although the single EF-hands form homodimers in the presence of Ca<sup>2+</sup>, the affinity between two EF1 peptides,  $\lg K = 5.21$ , is more than six orders of magnitude lower than the association constant for formation of heterodimer between EF1 and EF2,  $\lg K = 11.5$ . The heterodimerization constant was recently measured using surface plasmon resonance technology.<sup>36</sup> This enormous difference implies a very high specificity for heterodimers over homodimers in an EF1-EF2 mixture. In fact, the two EF-hands interact so tightly that they

resist separation by ion exchange in the presence of Ca<sup>2+</sup>.<sup>19,37</sup> The remarkable specificity for heterodimers is in line with other studies,<sup>37–40</sup> and was recently found to allow for dimerization of calbindin D<sub>9k</sub> via EF-hand swapping.<sup>41</sup>

#### Comparison to Intact Calbindin

EF-hand sites in intact proteins have affinities spanning a much wider range all the way up to  $10^9$  M<sup>-1</sup>. The Ca<sup>2+</sup>-binding constants obtained for EF1 and EF2 ( $\lg K = 4.4$ – $5.0$ ) are three to four orders of magnitude lower than those measured for intact calbindin D<sub>9k</sub> ( $\lg K = 7.8$ – $8.6$ )<sup>29</sup> under low ionic strength conditions. Hence, the specific contacts between the two EF-hands in the intact protein are crucial for maintaining its high Ca<sup>2+</sup> affinity. The inter EF-hand contacts favor an optimal arrangement of the Ca<sup>2+</sup> sites in the bound state and promote preformation of the sites in the apo state. Indeed, in the intact protein there is only a very small structural rearrangement upon Ca<sup>2+</sup> binding.<sup>42</sup> In the isolated EF-hand fragments, the free energy of Ca<sup>2+</sup> binding is reduced because a substantial energetic penalty is paid to drive a large conformational change.

We have shown that a series of Ca<sup>2+</sup> titrations at different peptide concentrations can be used to resolve the coupled Ca<sup>2+</sup>-binding and dimerization equilibria. The method can be used for other EF-hand fragments as well as for other systems where ligand binding and dimerization are coupled events. We find significant differences between the two EF-hands of calbindin D<sub>9k</sub>, with a higher dimerization tendency of the less charged EF1 fragment.

## ACKNOWLEDGMENTS

We thank Dr. Bertil Halle for the Levenberg-Marquardt fitting program LMFIT and for practical help in using and modifying it for this particular problem. We thank Andrea Ogard for assistance with CNBr cleavage and fragment purification.

## REFERENCES

- Kretsinger RH, Nockolds CEJ. Carp muscle calcium-binding protein. *J Biol Chem* 1973;248:3313–3326.
- Nakayama S, Moncrief ND, Kretsinger RH. Evolution of EF-hand calcium-modulated proteins. 2. Domains of several subfamilies have diverse evolutionary histories. *J Mol Evol* 1992;34:416–448.
- Reid RE, Gariépy J, Saund SK, Hodges RS. Calcium-induced protein folding. *J Biol Chem* 1981;256:2742–2751.
- Malik NA, Anantharamaiah GM, Gawish A, Cheung HC. Structural and biological studies on synthetic peptide analogues of a low-affinity calcium-binding site of skeletal troponin C. *Biochem Biophys Acta* 1987;911:221–230.
- Reid RE. Synthetic fragments of calmodulin calcium-binding site III. *J Biol Chem* 1990;265:5971–5976.
- Shaw GS, Hodges RS, Sykes BD. Probing the relationship between  $\alpha$ -helix formation and calcium affinity in troponin C:  $^1\text{H}$  NMR studies of calcium binding to synthetic and variant site III helix-loop-helix peptides. *Biochemistry* 1991;30:8339–8347.
- Tsuji T, Kaiser ET. Design and synthesis of the pseudo-EF hand in calbindin  $\text{D}_{9k}$ : effect of amino acid substitutions in the  $\alpha$ -helical region. *Proteins: Struct Func Gen* 1991;9:12–22.
- Procyshyn RM, Reid RE. A structure/activity study of calcium affinity and selectivity using a synthetic peptide model of the helix-loop-helix calcium-binding motif. *J Biol Chem* 1994;269:1641–1647.
- Reid RE, Procyshyn RM. Engineering magnesium selectivity in the helix-loop-helix calcium-binding motif. *Arch Biochem Biophys* 1995;323:115–119.
- Delbaere LTJ, Vandonselaar M, Reid RE. Crystallization of a synthetic analog of calcium-binding site III of rabbit skeletal troponin C. *J Biol Chem* 1989;264:10261–10263.
- Shaw GS, Hodges RS, Sykes BD. Calcium-induced peptide association to form an intact protein domain:  $^1\text{H}$  NMR structural evidence. *Science* 1990;249:280–283.
- Shaw GS, Hodges RS, Sykes BD. Determination of the solution structure of a synthetic two-site calcium-binding homodimeric protein domain by NMR spectroscopy. *Biochemistry* 1992;31:9572–9580.
- Kay LE, Forman-Kay JD, McCubbin WD, Kay CM. Solution structure of a polypeptide dimer comprising the fourth  $\text{Ca}^{2+}$ -binding site of troponin C by nuclear magnetic resonance spectroscopy. *Biochemistry* 1991;30:4323–4333.
- Revett SR, King G, Shabanowitz J, Hunt DF, Hartman KL, Laue TM, Nelson DJ. Characterization of a helix-loop-helix (EF hand) motif of silver hake parvalbumin isoform B. *Protein Sci* 1997;6:2397–2408.
- Chen JJ, Hong Y, Rustamzadeh E, Baleja JD, Androphy EJ. Identification of an  $\alpha$ -helical motif sufficient for association with papillomavirus E6. *J Biol Chem* 1998;273:13537–13544.
- Wendt B, Hofmann T, Martin SR, Bayley P, Brodin P, Grundström T, Thulin E, Linse S, Forsén S. Effect of amino acid substitutions and deletions on the thermal stability, the pH stability and unfolding by urea of bovine calbindin  $\text{D}_{9k}$ . *Eur J Biochem* 1988;175:439–445.
- Brodin P, Grundström T. Expression of bovine intestinal calcium binding protein from a synthetic gene in *Escherichia coli* and characterization of the product. *Biochemistry* 1986;25: 5371–5377.
- Johansson C, Brodin P, Grundström T, Thulin E, Forsén S, Drakenberg T. Biophysical studies of engineered mutant proteins based on calbindin  $\text{D}_{9k}$  modified in the pseudo EF-hand. *Eur J Biochem* 1990;187:455–460.
- Finn BE, Kordel J, Thulin E, Sellers P, Forsén S. Dissection of calbindin  $\text{D}_{9k}$  into two  $\text{Ca}^{2+}$ -binding subdomains by a combination of mutagenesis and chemical cleavage. *FEBS Lett* 1992;298:211–214.
- Laue TM, Shah BD, Ridgeway TM, Pelletier SL. Computer-aided interpretation of analytical sedimentation data for proteins. In: Harding SE, Rowe AJ, Horton JC, editors. Analytical ultracentrifugation in biochemistry and polymer science. Cambridge: The Royal Society of Chemistry; 1992. p 90–125.
- Marquardt DW. An algorithm for least-squares estimation of nonlinear parameters. *J Soc Indust Appl Math* 1963;11:431–441.
- Forsythe GE, Malcolm MA, Moler CB. Computer methods for mathematical computations. New York: Prentice-Hall; 1976.
- Donaldson C, Barber KR, Kay CM, Shaw GS. Human S100b protein: Formation of a tetramer from synthetic calcium-binding site peptides. *Prot Sci* 1995;4:765–772.
- Hirst JD, Brooks III CL. Helicity, circular dichroism and molecular dynamics of proteins. *J Mol Biol* 1994;243:173–178.
- Lakowicz JR. Principles of fluorescence spectroscopy. New York: Plenum Press; 1983.
- Akke M, Skelton NJ, Kordel J, Palmer AG III, Chazin WJ. Effects of ion binding on the backbone dynamics of calbindin  $\text{D}_{9k}$  determined by  $^{15}\text{N}$  NMR relaxation. *Biochemistry* 1993;32:9832–9844.
- Hofmann T, Eng S, Lilja H, Drakenberg T, Vogel HJ, Forsén S. Site-site interactions in EF-hand calcium-binding proteins. *Eur J Biochem* 1988;172:307–313.
- Andersson M, Malmendal A, Linse S, Ivarsson I, Forsén S & Svensson LA. Structural basis for the negative allosteric between  $\text{Ca}^{2+}$ - and  $\text{Mg}^{2+}$ -binding in the intracellular  $\text{Ca}^{2+}$ -receptor calbindin  $\text{D}_{9k}$ . *Prot Sci* 1997;6:1139–1147.
- Linse S, Johansson C, Brodin P, Grundström T, Drakenberg T, Forsén S. Electrostatic contributions to the binding of  $\text{Ca}^{2+}$  in calbindin  $\text{D}_{9k}$ . *Biochemistry* 1991;30:154–162.
- Svensson B, Jönsson B, Woodward C. Electrostatic contribution to the binding of  $\text{Ca}^{2+}$  in calbindin mutants. A Monte Carlo study. *Biophys Chem* 1990;38:179–183.
- Chazin WJ, Kordel J, Thulin E, Hofmann T, Drakenberg T, Forsén S. Identification of an Isoaspartyl Linkage Formed upon deamidation of bovine calbindin  $\text{D}_{9k}$  and structural characterization by 2D  $^1\text{H}$  NMR. *Biochemistry* 1989;28:8646–8653.
- Fast J, Håkansson M, Muranyi A, Gippert G, Thulin E, Evenäs J, Svensson LA, Linse S. Symmetric stabilization of bound  $\text{Ca}^{2+}$  ions in a cooperative pair of EF-hands through hydrogen bonding of coordinating water molecules in calbindin  $\text{D}_{9k}$ . *Biochemistry* 2001;40:9887–9895.
- Linse S, Thulin E, Sellers P. Disulfide bonds in homo- and heterodimers of EF-hand subdomains of calbindin  $\text{D}_{9k}$ : Stability, calcium binding, and NMR studies. *Prot Sci* 1993;2:985–1000.
- Linse S, Forsén S. Determinants that govern high-affinity calcium binding. *Adv Second Mess Phosphoprot Res* 1995;30:89–151.
- Shaw GS, Golden LF, Hodges RS, Sykes BD. Interactions between paired calcium-binding sites in proteins: NMR determination of the stoichiometry of calcium binding to a synthetic troponin-C peptide. *J Am Chem Soc* 1991;113:5557–5563.
- Berggård T, Julenius K, Ogard A., Drakenberg T, Linse S. Fragment complementation studies of protein stabilization by hydrophobic core residues. *Biochemistry* 2001;40:1257–1264.
- Linse S, Thulin E, Gifford LK, Radzewska D, Hagan J, Wilk RR, Akerfeldt KS. Domain organization of calbindin  $\text{D}_{28k}$  as determined from the association of six synthetic EF-hand fragments. *Prot Sci* 1997;11:2385–2396.
- Shaw GS, Findlay WA, Semchuk PD, Hodges RS, Sykes BD. Specific formation of a heterodimeric two-site calcium-binding domain from synthetic peptides. *J Am Chem Soc* 1992;114: 6258–6259.
- Durussel I, Luan-Rilliet Y, Petrova T, Tagaki T, Cox JA. Cation binding and conformation of typtic fragments of Nereis sarcoplasmic calcium-binding protein: calcium-induced homo- and heterodimerisation. *Biochemistry* 1993;32:2334–2400.
- Linse S, Voorhies M, Norström E, Schultz DA. A phage display study of calmodulin subdomain pairing. *J Mol Biol* 2000;296:473–486.
- Håkansson M, Fast J, Svensson LA, Linse S. An extended hydrophobic core induces EF-hand swapping. *Prot Sci* 2001;10:927–933.
- Skelton NJ, Kordel J, Chazin WJ. Determination of the solution structure of apo calbindin  $\text{D}_{9k}$  by NMR spectroscopy. *J Mol Biol* 1995;249:441–462.
- Svensson LA, Thulin E, Forsén S. Proline cis-trans isomers in calbindin  $\text{D}_{9k}$  observed by X-ray crystallography. *J Mol Biol* 1992;223:601–606.
- Koradi R, Billeter M, Wüthrich K. MOLMOL: a program for display and analysis of macromolecular structures. *J Mol Graph* 1996;14:51–55.